



## Numerical Analysis of Key Parameters Influencing the Replacement of a Shell-and-Tube Heat Exchanger with an Automotive Radiator

Amin Eskandari | Faramarz Ranjbar\*  | Moharram Jafari | Faramarz Talati

Department of Mechanical Engineering, University of Tabriz, Tabriz, Iran

\* Corresponding author, Email: [s.ranjbar@tabrizu.ac.ir](mailto:s.ranjbar@tabrizu.ac.ir)

### Article Information

#### Article Type

RESEARCH ARTICLE

#### Article History

RECEIVED: 15 Aug 2025

REVISED: 17 Oct 2025

ACCEPTED: 09 Dec 2025

PUBLISHED ONLINE: 05 Jan 2026

#### Keywords

Compact heat exchanger  
Shell-tube heat exchanger  
Dynamic analysis  
Radiator

### Abstract

A radiator is a crucial component of an engine's cooling system. It circulates a mixture of water and antifreeze, releasing heat as it draws in cooler air before the fluid returns to the engine. One common issue concerning radiators is their mounting location, which can vary across different automobile models. In automobiles and trucks, the radiator is typically mounted at the front, making it highly susceptible to damage in front-end collisions. Such damage often leads to coolant leakage, which can result in further impairment of the vehicle's engine and cooling system. This report aims to introduce a new system, utilizing a shell-and-tube heat exchanger, as an alternative to the conventional radiator while fulfilling its cooling function. The proposed approach addresses the limitations of traditional radiators and offers improvements in both thermal capacity and safety. This study presents a low-error simulation of the OM457-946 diesel engine, manufactured by IDEM Tabriz Company, incorporating both a test report and an accurate performance curve. The heat load values are 65.31 kW at no-load and 900 rpm, and 120.95 kW at full engine load and 2000 rpm. The engine's power output and thermal efficiency were analyzed at various speeds, revealing that replacing the shell-and-tube heat exchanger with an automotive radiator increases the cooling system's volume and resistance. This modification results in a 2% increase in engine power and a 7% improvement in thermal efficiency.

**Cite this article:** Eskandari, A., Ranjbar, F., Jafari, M., Talati, F. (2026). Numerical Analysis of Key Parameters Influencing the Replacement of a Shell-and-Tube Heat Exchanger with an Automotive Radiator. DOI: [10.22104/hfe.2025.7457.1347](https://doi.org/10.22104/hfe.2025.7457.1347)



© The Author(s).

DOI: [10.22104/hfe.2025.7457.1347](https://doi.org/10.22104/hfe.2025.7457.1347)

Publisher: Iranian Research Organization for Science and Technology (IROST)

---

## 1 Introduction

A radiator is a heat exchanger designed to transfer thermal energy between two media for the purpose of heating and cooling. Radiators are widely used in automobiles, buildings, and electronics devices. A radiator continuously transfers heat to its surrounding environment to either warm it up or cool the fluid or coolant it contains, as observed in car engine cooling systems and HVAC dry cooling towers. In spite of the term, most radiators actually transmit heat through convection rather than thermal radiation.

Radiators are employed to cool internal combustion engines, primarily automobiles but also in piston aircraft engines, locomotive engines, motorcycles, stationary power plants, and other heat engine applications. Boats typically employ liquid-liquid heat exchangers since they have access to a large supply of relatively cool external water. In contrast, the radiator in most road vehicles is particularly vulnerable to damage in road accidents due to its frontal position. Redesigning and relocating the radiator with a heat exchanger is a viable solution to prevent radiator damage in accidents. A heat exchanger is a device used to transfer thermal energy from a heat source to a working fluid.

Heat exchangers are used for both cooling and heating applications. The fluids involved may be separated by a solid barrier to prevent mixing or may come into direct contact, depending on the design. Heat exchangers are widely used in space heating, refrigeration, air conditioning, power generation, chemical and petrochemical processing, petroleum refining, natural gas processing, and wastewater treatment. A common example of a heat exchanger is found in an internal combustion engine, where a circulating fluid – known as engine coolant – flows through the radiator's coils. As air passes over these coils, the coolant is cooled while the air is warmed through heat transfer. A heat sink is a passive heat exchanger that dissipates heat produced by an electrical or mechanical device to a fluid medium, typically air or a liquid coolant. In contrast, a shell-and-tube heat exchanger offers greater flexibility in mounting location and typically uses a radial fan instead of an axial fan to enhance airflow and cooling efficiency.

This shaft can be directly connected to the engine's water pump shaft or driven by a separate electric motor. Since the pressure drop across the proposed heat exchanger is well within the capabilities of typical engine centrifugal pumps – which operate at a head pressure of approximately 6 psi – radial fans are suitable, offering a maximum head development of around 300 millimeters of water. Under no-load conditions, when

the vehicle is stationary, the primary limitation is the pressure drop of air flowing through the heat exchanger; therefore, future improvements in this area hold significant potential. During vehicle motion and rising engine RPM, the initial head rise is estimated using the similarity principles of incompressible flow in turbomachinery. Additionally, the dynamic pressure of the airflow entering the engine compartment can be considered. At high speeds and low ambient temperatures, the assumption of incompressible airflow remains valid, as the Mach number stays below 0.3.

For heavy trucks that run at higher torque and low speeds, the original radiator size can still be used, even with the addition of an air-conditioning condenser, to compensate for the pressure drop across the heat exchanger, filters, and air duct passages.

The airflow generated by the truck's motion can be directed and shaped using an air duct, which can be resized accordingly. This design helps generate sufficient dynamic head before the air reaches the fan, even while maintaining the permissible flow velocity. The fan then contributes additional head, accounting for the total pressure differential across the system. The results of these calculations will be presented in tables and graphs, followed by analysis and conclusions.

Heat exchangers are among the most often utilized components in physical and chemical processes. They are commonly observed in the majority of industrial facilities. This operation can occur between liquid-liquid, gas-gas, or gas-liquid phases. Heat exchangers are employed in numerous applications. These applications encompass span a wide range of industries, including power generation, refineries, petrochemicals, construction and manufacturing, process industries, food and pharmaceuticals, metal smelting, heating, ventilation, air conditioning, refrigeration, and aerospace. Numerous apparatuses, including boilers, steam generators, condensers, evaporators, coolers, cooling towers, preheaters for fan coil units, oil coolers, heaters, radiators, and furnaces, are classified as heat exchangers [1]. Heat exchangers are critical components in power plants and refineries, where they play a vital role in regulating the temperature of industrial fluids. In refineries, a distillation column typically includes multiple heat exchanger. The significance of heat exchangers lies in their ability to maintain the required temperature conditions of process fluids. Failure to achieve this can disrupt the operation of the refinery or any industrial or chemical facility [2]. The diverse applications of high-pressure heat exchangers necessitate the examination and analysis of their special properties in comparison to other types, from an engineering standpoint. This section will review various studies conducted in the domain of heat exchangers. Shell and tube heat exchangers can

be categorized according to several criteria: (1) Classification and Contact Interface of Heated and Chilled Fluids; (2) Direction of Flow for Hot and Cold Fluids; (3) Mechanism of Heat Transfer Between Fluids; (4) Mechanical Design and Fabrication of Exchangers [3]. Shell and tube heat exchangers are the most commonly used non-fired heat transfer devices across various industries. Their distinctive construction enables them to endure elevated pressures and temperatures beyond 30 bar and 260 °C. The tubes, either finned or plain, are aligned parallel to the shell's longitudinal axis. The exchanger consists of a cylindrical shell that houses these tubes, enabling efficient heat transfer between fluids. The tubes are affixed at both ends to perforated plates called tube sheets and pass through a series of plates known as baffles. These baffles direct the shell-side fluid to flow perpendicular to the tubes, enhancing heat transfer. The combination of tubes and baffles is known as the tube bundle. The tube bundle is held in place by tie rods and spacers. Fluid enters and exits the tubes through specialized components known as fixed heads and floating heads, which are sometimes also referred to as inlet and outlet heads [4]. The selection of heat exchanger type is contingent upon criteria such as cleaning accessibility, anticipated temperature differentials, and the implications of thermal expansion and contraction on the tube bundle, shell, and internal connections. Boot et al. examined a coil heat exchanger subjected to abrupt variations in water flow rate and formulated expressions for its time constant [5]. Pearson investigated a double-pipe heat exchanger with abrupt variations in the inlet temperature of one fluid stream [6].

Heidi analyzed a similar scenario with incremental variations in the inlet temperature of both water and air streams. He derived the governing equations and examined the impact of these alterations on temperature and flow rate [7]. Ratzle and Schwan employed several flow distribution models on the shell side to examine the transient response of a heat exchanger resulting to step changes in the inlet temperature of both fluids. They evaluated both co-current and counter-current flow arrangements [4]. The governing equations were resolved with the Laplace transform. The research investigated the impact of irregular flow distribution adjacent to the shell walls and the thermal inertia of the shell walls on the system's transient behavior. The Nusselt number ( $Pe$ ) quantifies the effects of non-uniform flow distribution. This effect persists throughout time, although its impact diminishes beyond a specific threshold time ( $z$ ). This threshold is contingent upon characteristics such as the Nusselt number ( $Pe$ ), the Number of Transfer Units (NTU), and others [8]. Ataer et al. investigated the dynamic

behavior of finned-tube heat exchangers. They examined the impact of a sudden alteration in water inlet temperature on the exchanger's response utilizing three different methodologies. In the initial approach, they disregarded the thermal capacity of the fins and tube walls.

In Method 2, it was assumed that the heat capacities of both components were identical, whereas in Method 3, the heat capacities of the fins and tube walls were evaluated independently. Assuming a constant thermal gradient between the inlet and outflow of both fluids, the researchers employed energy conservation equations and resolved them numerically for incremental variations in water inlet temperature. Subsequently, they juxtaposed the outcomes from each strategy with empirical data. The outcomes derived from Method 3, which accounted for various heat capacities, most closely aligned with the experimental data [9]. In a separate study, they examined time delay and the duration required to attain a steady state, offering a methodology to assess the transient performance of the heat exchanger in response to variations in inlet air temperature, air velocity, and water flow rate. Furthermore, they examined the transient dynamics of finned-tube heat exchangers employing an approximation methodology [10]. Sharifi et al. examined the transient dynamics of a plate-and-frame heat exchanger experiencing abrupt alterations in water inlet temperature. They used a lumped parameter model to simulate temperature distributions across the flow channels within the exchanger. The outcomes derived from this model were juxtaposed with experimental data under both steady-state and transient situations. The lumped parameter model developed by the researchers provides a generalized approach for analyzing the transient behavior of diverse plate-and-frame heat exchangers, irrespective of their dimensions [11].

Grittoff et al. performed a comparative analysis of steady-state and transient techniques for assessing local heat transfer in flat finned-tube heat exchangers [12]. The results acquired under steady-state circumstances were more aligned with numerical expectations [12]. Lou and Ratzlaff investigated the transient dynamics of finned-plate heat exchangers in response to abrupt variations in fluid temperatures. They derived the governing equations, non-dimensionalized them, and solved them using the Laplace transform method. In aluminum finned-plate heat exchangers, the transverse thermal resistance within the fins was considered insignificant. The authors indicated that the solution method could be used to many types of heat exchangers and that the governing equations would be simpler for non-finned heat exchangers [13]. Ranong and Ratzlaff examined the steady-state and transient dynamics of

two interconnected heat exchangers featuring distinct inlet and outlet flow configurations. The Laplace transform approach was utilized to examine and resolve the impact of flow rate and inlet temperature fluctuations on heat exchanger performance. Their findings indicated that in plate-fin heat exchangers, the fins and separator plates have unique transient thermal characteristics, resulting in lateral heat conduction within the fins [14]. Ribeiro et al. proposed a numerical solution for the steady-state simulation of plate heat exchangers (PHEs). Their approach accounts for many configurations in which the hot and cold streams flow in counter-current, concurrent, or a combination of these patterns, arranged either in series or parallel. They juxtaposed numerical outcomes with analytical solutions for simple scenarios and empirical data. The authors effectively implemented their algorithm to model an industrial PHE utilized for milk pasteurization, showcasing

the efficacy of their method [15].

This study indicates that the reinforced water tank and enhanced cooling system of the vehicle are bound to increase the efficiency and power of the engine. Thus, this article aims to numerically assess the extent of improvement in thermal efficiency and engine performance.

## 2 Methods

Table 1 summarizes the Euro IV engine test results for OM456 type 649 and 945 engines, manufactured by IDeM Tabriz under license from Daimler-Chrysler Germany. Based on these results, the following engine heat loads will be used for subsequent calculations: No-load condition: 3125 kW at 900 RPM Full-load condition: 9513 kW at 2000 RPM.

**Table 1. Summary of test report for engine heat load**

| Motor type  | RPM  | Torque (N.m) | Power (kW) | Specific fuel consumption (gr/kW.hr) | Fuel consumption mass flow rate (kg/s) | Heat Production (kW) | Thermal efficiency (%) | Cooling water Heat (kW) |
|-------------|------|--------------|------------|--------------------------------------|--|----------------------|------------------------|-------------------------|
| OM457 (956) | 900  | 1260         | 118.7      | 200                                  | 0.006                                  | 276.5                | 42.95                  | 65.31                   |
|             | 1300 | 1250         | 170.1      | 194                                  | 0.009                                  | 384.1                | 44.29                  | 93.59                   |
|             | 1700 | 1210         | 215.4      | 198                                  | 0.011                                  | 496.3                | 43.10                  | 118.5                   |
|             | 2000 | 1050         | 219.9      | 223                                  | 0.013                                  | 570.7                | 38.53                  | 120.9                   |

**Table 2. Test Results of Cooling water returning to engine (radiator outlet)**

| RPM           | 1 <sup>st</sup> test | 2 <sup>nd</sup> test | 3 <sup>rd</sup> test | 4 <sup>th</sup> test | 5 <sup>th</sup> test | Average |
|---------------|----------------------|----------------------|----------------------|----------------------|----------------------|---------|
| 900           | 79.00                | 76.00                | 73.50                | 74.40                | 74.10                | 75.40   |
| 1300          | 77.50                | 76.35                | 76.00                | 74.45                | 74.35                | 75.73   |
| 1700          | 76.70                | 77.96                | 75.90                | 76.72                | 74.7                 | 76.40   |
| 2000          | 78.00                | 78.20                | 77.80                | 77.50                | 75.00                | 76.50   |
| Total Average |                      |                      |                      |                      |                      | 76.033  |

A full test report of the above-mentioned engine is provided in the appendix. The report includes a sample of 5 rows selected from a total of 30 data entries. Each row has 16 columns, representing different engine performance parameters. The test results were acquired through AVL's test process conducted in a test cell at the engine builder's location and can be considered as a "performance test." The data presented in Table 1 is extracted from this test report. The appendix also includes another document outlining the performance specifications for two types of OM457 engines. It features graphs illustrating graphs of brake power, brake torque, and specific fuel consumption as functions of engine speed.

Table 2 presents the test results for the radiator

outlet water temperature and the engine return water. The table contains the data for five test runs of engine performance at four engine speeds. The average temperatures for each engine speed are computed and presented in the table.

From Table 2, the mean return engine coolant temperature is 76.033 degrees Celsius. While this value is partially influenced by the test cell ambient conditions, it closely aligns with the reference temperature of 170 °F, with a deviation of less than 1%.

## 3 Governing Equations

The water flow rate will be determined by the conservation of energy in a steady state, based on the average

standard inlet and outlet temperatures of the engine coolant and water properties from appropriate tables.

$$Q_{cc} = m_0 C_{pw} \Delta T_w \quad (1)$$

Table 3 compares the measured volumetric water flow rate from the test cell with the values calculated using Equation (2). The table shows a minimal relative error between the two sets of data, indicating strong agreement between the experimental measurements and the computational approach.

Because the critical heat transfer condition for the heat exchanger is at engine idle speed (900 rpm), the lowest permissible velocities of the hot fluid (water) and

the cold fluid (air) should be taken into account [3].

$$V_w = V_w A_c = V_w N_t \frac{\pi}{4} D^2, \quad (2)$$

$$h_i = 5.678 (0.913 - 0.42 \log D_i^2) \times (165 + 1.7 t_m) V_{fps}^{0.805}. \quad (3)$$

Based on Table 4, displaying the heat exchanger specifications of the tubes from relevant standard tables, the aforementioned equations will be employed to calculate the number of tubes in each water passageway, the effective velocity of water within the tubes (accounting for non-uniform flow distribution), and the convective heat transfer coefficients – representing the rate of heat transfer between the water and the inner surface of the tubes.

**Table 3. Test Results for Cooling water mass flow rate and heating load**

| Motor type | RPM  | Heat Load (kW) | Calculated mass flow rate of cooling water (kg/s) | Calculated volumetric flow rate of cooling (kg/s)water | measured mass flow rate of cooling water (kg/s) | Relative error (%) |
|------------|------|----------------|---|--|---|--------------------|
| OM457(945) | 900  | 65.31          | 2.799   | 2.8817   | 2.88  | 0.0342             |
|            | 1300 | 93.59          | 4.011   | 4.1295   | 4.130   | 0.0345             |
|            | 1700 | 118.47         | 5.075   | 5.2273   | 5.229   | 0.0340             |
|            | 2000 | 120.95         | 5.187   | 5.3365   | 5.338   | 0.0348             |

**Table 4. Number of tubes in one pass and convection heat transfer coefficient dependent on tube diameter**

| The outer diameter of the tube (in) | BWG <sup>1</sup> | Thickness of tubes | Inner diameter of pipes (in) | Number of tubes | Modified velocity (fps) | Heat transfer coefficients (W/m <sup>2</sup> K) | AHt/L (in <sup>2</sup> /in) |
|-------------------------------------|------------------|--------------------|------------------------------|-----------------|-------------------------|---|-----------------------------|
| 6/8                                 | 18               | 0.049              | 0.65                         | 11              | 3.99                    | 7930.5  | 25.90                       |
| 5/8                                 | 19               | 0.042              | 0.54                         | 16              | 3.98                    | 8193.4  | 31.38                       |
| 4/8                                 | 20               | 0.035              | 0.43                         | 25              | 4.03                    | 8617.8  | 39.25                       |
| 3/8                                 | 20               | 0.035              | 0.30                         | 50              | 4.01                    | 9078.4  | 58.9                        |
| 2/8                                 | 20               | 0.028              | 0.19                         | 124             | 3.99                    | 9715.5  | 97.36                       |

The following calculations show that the air-side convection coefficient is inferior to the water-side convection coefficient. The air side is the controlling layer for heat transfer. As a result, the selection of tube size will not significantly affect the overall heat transfer coefficient of the heat exchanger. Therefore, the attention should focus on reducing the heat transfer surface area. The examination of the last column in Table 4, which represents the heat transfer area per unit length per pass with a uniform tube spacing factor, indicates an interesting correlation. The width of the heat exchanger will be identical for a given heat transfer area, irrespective of the tube diameter selected. Hence, the selection of tube diameter can be based on the allowable pressure drop for the airflow. Essentially, as long as the total heat transfer area remains con-

stant, a heat exchanger with a wider configuration and smaller-diameter tubes can perform equivalently to a narrower exchanger with larger-diameter tubes. However, using smaller tubes increases the pressure drop on the air side. The determination of the required airflow rate is subsequently based on the specified inlet and outlet air temperatures.

$$Q = m_a C_{pa} \Delta T_a, \quad (4)$$

$$C_n = m_w C_{pw}, \quad (5)$$

$$C_c = m_a C_{pa}, \quad (6)$$

$$C = \frac{C_{\min}}{C_{\max}}, \quad (7)$$

$$\varepsilon = \varepsilon_c = \frac{t_2 - t_1}{T_1 - t_1}. \quad (8)$$

<sup>1</sup>Birmingham Wire Gauge

The ratio between the cold fluid's heat capacity flow rate and the temperature flow rate, or the thermal efficiency, for a flow where the cold fluid has the minimum heat capacity.

$$Ntu = -\frac{1}{c} \ln [1 + C \ln(1 - \varepsilon)], \quad (9)$$

$$u_A = Ntu C_{\min}. \quad (10)$$

The following calculation demonstrates that, under optimal heat exchanger capacity conditions and ample heat transfer area, the most optimal option is a 4/3-inch pipe with brief integral fins consisting of 19 fins per inch and an internal diameter of 14 millimeters. The baseline specifications before and after finning are given in Table 5.

**Table 5. Tube specification without fin**

| O.D  |      | BWG | L    |      | I.D  |      | OD/ID |
|------|------|-----|------|------|------|------|-------|
| Inch | mm   |     | Inch | mm   | Inch | mm   |       |
| 3/4  | 19.0 | 18  | 0.04 | 1.24 | 0.65 | 16.5 | 1.15  |

**Table 6. Finned tube specification**

| Manufacturer classification | T(mm) | H(mm) | Di(mm) | FRI | Aof/Ai |
|-----------------------------|-------|-------|--------|-----|--------|
| MLF1919135                  | 1.35  | 1.175 | 14     | 19  | 3.5    |

## 4 Validation

Given that almost no similar work has been done on this subject, to validate this design, a dimensionless parameter, the Reynolds number, was used in the heat exchanger and its results were compared with those reported by R. Gugulothu and N. Sanke [16].

The results showed acceptable overlap, with a calculated error percentage of 0.53%.

## 5 Results

Based on the radiator window dimensions for trucks with power above 100 kW and the radiator thickness, the core volume is approximately 118,800 cubic centimeters. In contrast, the proposed heat exchanger has a significantly smaller core volume of 5,975 cubic centimeters.

According to the calculations performed and the technical specifications of Idem Tabriz Company, Table 7 presents a comparison between the designed heat exchanger dimensions and those of the radiator.

This comparison clearly shows that the dimensions of the heat exchanger designed in this study are 46% smaller than those of car radiators. Calculations were based on a maximum allowable airflow velocity of 40 meters per second and a maximum allowable water flow velocity of 8 feet per second (fps). The results for both no-load and full-load engine conditions are summarized and compared in Table 8.

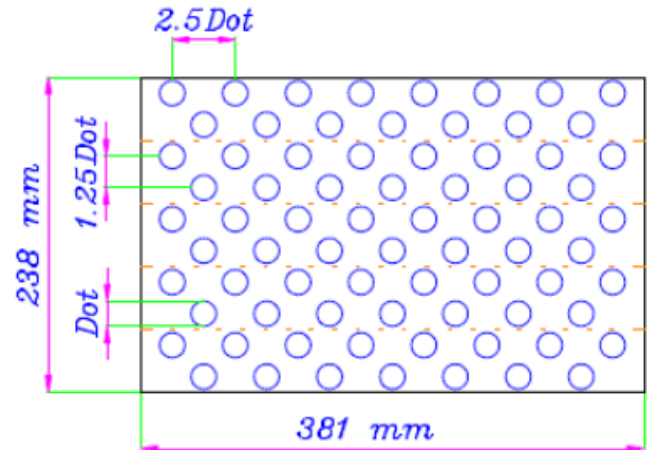


**Fig. 1. Geometric specification of the heat exchanger plate**

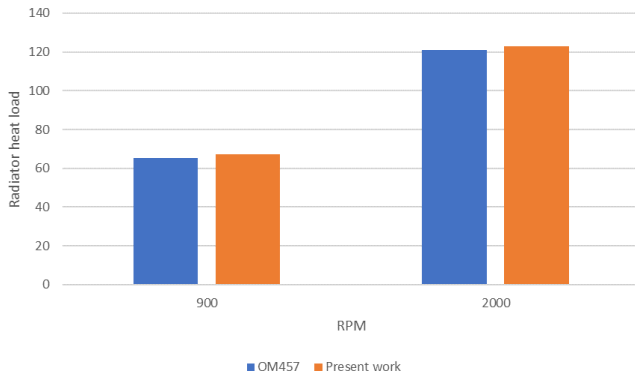
**Table 7. Comparing the designed heat exchanger with radiator**

|                       | Length (cm) | Height (cm) | Width (cm) | Volume (cm <sup>3</sup> ) |
|-----------------------|-------------|-------------|------------|---------------------------|
| Radiator              | 12          | 120         | 75         | 108000                    |
| Rectangular Cube H.E. | 64          | 24          | 38         | 58368                     |

Also Figure 2 compare the Radiator Heat Load between OM457 and present work. The system under study is a heat exchanger designed to improve thermal efficiency, with calculations indicating an increase of approximately 7%.

**Table 8. The results of no load and a full load of the engine**

| Type of engine | RPM  | Radiator Heat Load (kW) | Air Mass Flow Rate (kg/s) | Maximum Velocity of air (m/s) | Air Inlet temperature | Outlet Air Temperature | Pressure Drop in Air Flow Rate | Total Pressure Drop (mm wG) |
|----------------|------|-------------------------|---------------------------|-------------------------------|-----------------------|------------------------|--------------------------------|-----------------------------|
| OM457          | 900  | 65.31                   | 4.33                      | 25                            | 25                    | 40                     | 85                             | 287.3                       |
|                | 2000 | 120.9                   | 6.93                      | 40                            | 25                    | 42.35                  | 202                            | 720.0                       |
| Present Work   | 900  | 67.2                    | 5.5                       | 22                            | 21                    | 40                     | 83                             | 288                         |
|                | 2000 | 123                     | 8                         | 37                            | 21                    | 41                     | 200                            | 721                         |

**Fig. 2. Comparing radiator heat load**

## 6 Conclusion

The designed heat exchanger has a core volume of 59,575.5 cubic centimeters, whereas the core volume of radiators in trucks with power above 100 kW is

approximately 118,800 cubic centimeters, based on the radiator window dimensions and thickness. This means the total volume of the cooler, including the upper and lower temperature headers, is approximately 147,690.0 m<sup>3</sup>, while the volume of the proposed exchanger, including the water flow headers and air flow conversion ducts, is approximately 124,053.6 cm<sup>3</sup>.

Given that the fan's static pressure (production head) is 300 mm WG, when the engine operates at full load, an additional pressure drop of approximately 420 mm WG occurs due to the increased speed and heat load of the radiator-replacement exchanger. This additional pressure must be compensated by the vehicle's dynamic pressure generated by its speed. For instance, at a speed of 60 km/h, about 17.7% of the radiator window height would need to be utilized for airflow. The key novelty of the present study lies in modifying and optimizing the radiator's shape and volume, thereby enhancing its structural strength and physical resistance during accidents.

## Nomenclature

|                   |  |
|-------------------|--|
| $C_p$             | Specific heat, JkgK <sup>-1</sup>                                |
| $d_f$             | Diameter of the base fluid molecule, m                           |
| $d_p$             | Diameter of the nanoparticle, m                                  |
| $g$               | Gravitational acceleration, ms <sup>-2</sup>                     |
| $H$               | Enclosure height, m  |
| $\bar{h}$         | Heat transfer coefficient, Wm <sup>-2</sup> K <sup>-1</sup>      |
| $L$               | Enclosure length, m  |
| $k$               | Thermal conductivity, WmK <sup>-1</sup>                          |
| $k_b$             | Boltzmann's constant   |
| $\overline{Nu}_i$ | Average Nusselt number on the walls of the each heater or cooler |
| $Nu_{tot}$        | Sum of Nu, of all heaters or coolers                             |
| $P$               | Pressure, Nm <sup>-2</sup>                                       |
| $T$               | Temperature, K   |
| $T_{fr}$          | Freezing point of the base fluid, K                              |
| $u, v$            | Velocity components, ms <sup>-1</sup>                            |
| $u_B$             | Brownian velocity of the nanoparticle, ms <sup>-1</sup>          |
| $u, v$            | Dimensionless velocity components                                |
| $x, y$            | Cartesian coordinates, m   |

$X, Y$  Dimensionless Cartesian coordinates

### Greek symbols

|          |  |
|----------|--|
| $\alpha$ | Thermal diffusivity, m <sup>2</sup> s <sup>-1</sup>  |
| $\beta$  | Thermal expansion coefficient, K <sup>-1</sup>       |
| $\theta$ | Dimensionless temperature                            |
| $\mu$    | Dynamic viscosity, kgm <sup>-1</sup> s <sup>-1</sup> |
| $\nu$    | Kinematic viscosity, m <sup>2</sup> s <sup>-1</sup>  |
| $\rho$   | Density, kgm <sup>3</sup>                            |

## References

- [1] Horniyk K. Heat Exchangers-Thermal-Hydraulic Fundamentals and Design. Nuclear Technology. 1982;58(3):556-6.
- [2] Costa AL, Queiroz EM. Design optimization of shell-and-tube heat exchangers. Applied thermal engineering. 2008;28(14-15):1798-805.
- [3] Shah R, Sekulic D. Heat exchangers. Handbook of heat transfer. 1998;3.

- [4] Shah RK, Sekulic DP. Fundamentals of heat exchanger design. John Wiley & Sons; 2003.
- [5] Boot J, JT P, RG L. An Improved Dynamic Response Model for Finned SERPENTINE CROSS-FLOW HEAT EXCHANGERS. ASHRAE Trans. 1977:218-39.
- [6] Pearson JT, RG L, RD M. Gain and time constant for finned serpentine crossflow heat exchangers. ASHRAE Trans. 1974:255-67.
- [7] Haidi M, Padet J. Study of a heat exchanger with variable inlet. Universite de pau et des payes del Adour; 1991.
- [8] Roetzel W, Xuan Y. Analysis of transient behaviour of multipass shell and tube heat exchangers with the dispersion model. International journal of heat and mass transfer. 1992;35(11):2953-62.
- [9] Ataer ÖE, Ileri A, Göğüş Y. Transient behaviour of finned-tube cross-flow heat exchangers. International journal of refrigeration. 1995;18(3):153-60.
- [10] Ataer ÖE. An approximate method for transient behavior of finned-tube cross-flow heat exchangers. International journal of refrigeration. 2004;27(5):529-39.
- [11] Sharifi F, Narandji MG, Mehravaran K. Dynamic simulation of plate heat exchangers. International Communications in Heat and Mass Transfer. 1995;22(2):213-25.
- [12] Critoph R, Holland M, Fisher M. Comparison of steady state and transient methods for measurement of local heat transfer in plate fin-tube heat exchangers using liquid crystal thermography with radiant heating. International journal of heat and mass transfer. 1999;42(1):1-12.
- [13] Luo X, Roetzel W. The single-blow transient testing technique for plate-fin heat exchangers. International journal of heat and mass transfer. 2001;44(19):3745-53.
- [14] Ranong CN, Roetzel W. Steady-state and transient behaviour of two heat exchangers coupled by a circulating flowstream. International journal of thermal sciences. 2002;41(11):1029-43.
- [15] Ribeiro Jr C, Andrade MC. An algorithm for steady-state simulation of plate heat exchangers. Journal of food engineering. 2002;53(1):59-66.
- [16] Gugulothu R, Sanke N. Experimental investigation of heat transfer characteristics for a shell and tube heat exchanger. Energy Harvesting and Systems. 2024;11(1):20220147.